Transportation Research Part D 65 (2018) 438–457

Contents lists available at ScienceDirect

Transportation Research Part D

journal homepage: www.elsevier.com/locate/trd

Static green repositioning in bike sharing systems with broken bikes

Yue Wang, W.Y. Szeto*

Department of Civil Engineering, The University of Hong Kong, Pokfulam Road, Hong Kong
The University of Hong Kong, Shenzhen Institute of Research and Innovation, Shenzhen, China

A B S T R A C T

Bike-Sharing Systems (BSSs) and environmental concerns have been receiving increasing popularity in transportation operations. In BSSs, the distribution of bike demand often mismatches with bike supply and there are broken bikes. Usable bikes are needed to redistribute between stations to satisfy the demand and all broken bikes need to be carried back to the depot for repairs. Both types of bikes are often transported by fossil-fueled vehicles but using these vehicles for the operation may damage the environmental creditability of BSSs. A methodology is needed to mitigate the environmental impact of this operation.

This study aims to propose a methodology to reposition both good and broken bikes in a bike-sharing network in order to achieve a perfect balance between bike demand and supply at each station and make sure that all broken bikes are moved back to the depot. The objective of this repositioning operation is to minimize the total CO_2 emissions of all repositioning vehicles. A Mixed Integer Linear Program (MILP) model is presented to formulate the problem mentioned above and a commercial solver is used to solve it for small applications. Using example applications, problem characteristics and the factors that affect the CO_2 emissions are discussed. The results indicate that allowing multiple visits can reduce vehicle emissions. Moreover, when the percentage of broken bikes in the system increases, the CO_2 emissions increase. Furthermore, if there is a tolerance for meeting the demand target, when this tolerance increases, the CO_2 emissions decrease. In addition, when the distance of a link in an optimal route increases, the resultant emissions may remain unchanged. Besides, when the vehicle capacity increases, the CO_2 emissions decrease. The real world instances of Citybike Vienna are used to compare emission and distance minimization solutions and investigate the runtime complexity of the proposed model. The results demonstrate that a shorter distance may not necessarily lead to lower emissions. The results also show that as the number of vehicles increases, the total emissions and runtime increase. A clustering method based on the nearest neighbor heuristic together with a commercial solver is used to solve a large real-world instance. This result confirms the possibility of using the clustering approach to reduce the running time for large network instances with multiple vehicles.

1. Introduction

Cycling is an environment-friendly and healthy transport mode. It has received increasing attention in recent years. To encourage cycling, many cities have introduced public BSSs such as Velib in Paris, Villo in Brussels, Citi-Bike in New York City, and Santander Cycles in London. As of 16 September 2018, public BSSs were available in about 1780 cities (Meddin and DeMaio, 2018). In a classical BSS, registered users can rent a bike at a bike station, ride the bike, and return it to any station. Due to the asymmetrical distribution of bike flows, the deficient supply of both lockers and bikes often occur in these systems. The former situation leads to extra travel distances for some bike users to find available lockers while the latter one causes unsatisfied demand. To cater to the demands for both lockers and bikes, bike repositioning is essential.

In general, there are two types of bike repositioning: static and dynamic. Static bike repositioning (e.g., Li et al., 2016; Cruz et al., 2017; Ho and Szeto, 2017; Schuijbroek et al., 2017) usually focuses on the nighttime repositioning because, during that time, system

* Corresponding author.
E-mail addresses: yuewhku@hku.hk (Y. Wang), ceszeto@hku.hk (W.Y. Szeto).

https://doi.org/10.1016/j.trd.2018.09.016

Available online 27 September 2018

usage and the congestion impact can be ignored. The target is to meet the demands in the next morning. Dynamic bike repositioning concerns with the daytime situation when the system is in high usage and the demand of each station will change during the repositioning period (e.g., Caggiani and Ottomanelli, 2012; Contardo et al., 2012; Kloimüllner et al., 2014; Ghosh et al., 2017; Caggiani et al., 2018; Shui and Szeto, 2018). Both types of repositioning can be found in practice.

Both types of bike repositioning are commonly performed by fossil-fueled vehicles. Using these vehicles for the operation may damage the environmental creditability of BSSs (Wiersma, 2010) because these vehicles emit pollutants and greenhouse gases. Other than the unmet demands for both lockers and bikes, environmental objectives should be duly considered in the repositioning operation. However, in the literature, except Shui and Szeto (2018), environmental objectives are rarely considered in bike repositioning studies.

Another important consideration is broken bikes. Broken bikes are regularly found in BSSs (Kaspi et al., 2016, 2017). The presence of broken bikes in the systems means not only a waste of resources but also causes user dissatisfaction. Broken bikes occupy lockers and reduce the parking spaces for users to return bikes. Moreover, broken bikes cannot be used to satisfy bike users' demand. In addition, broken bikes are always transported back to depots for repairs and use up some of the capacity of repositioning vehicles for usable bikes, making the repositioning of usable bikes less effective. It is therefore important to consider the repositioning of both usable and broken bikes simultaneously. However, no studies, except Alvarez-Valdes et al. (2016), considered this type of repositioning. Moreover, to the best of our knowledge, no studies simultaneously considered both broken bikes and an environmental objective at the time of this writing.

In this paper, we study a static green Bike Repositioning Problem (BRP) in the presence of broken bikes. This problem determines the route and the corresponding loading or unloading instructions for each repositioning vehicle to balance a BSS with broken bikes. The objective is to minimize the total CO_2 emissions of all the vehicles. An MILP model is proposed to formulate the problem, which is then solved using a commercial solver. Numerical experiments are carried out on small example networks to clearly illustrate the problem characteristics and investigate the factors that affect the vehicle emissions. The real world instances of Citybike Vienna are also used to compare emission and distance minimization solutions and investigate the runtime complexity of the proposed model. A clustering method based on the nearest neighbor heuristic and a commercial solver is used to solve the large real-world instance with 90 stations. The computational time required and solution quality obtained by this method are also demonstrated.

The contributions of this paper lie on the following:

1. to introduce a new and practical BRP—a static green BRP with broken bikes;
2. to present a model to formulate the problem, and;
3. to illustrate the problem properties and point out critical factors that affect vehicle emissions.

The remainder of the paper is organized as follows. Section 2 reviews the literature on BRPs and fuel consumption and CO_2 emission modeling. Section 3 presents a mathematical model for the studied problem. Section 4 describes the numerical studies and discusses the results. Section 5 discusses different approaches to solving large-scale BRPs. Finally, Section 6 concludes this paper and gives future research directions.

2. Literature review

In this section, we will first briefly introduce the objectives used in BRPs. Moreover, we will describe how current research addresses the fuel consumption and CO_2 emissions, especially the factors considered in mathematical models. Afterward, we will discuss the literature about broken bikes and the modeling assumptions in BRPs. Finally, we will depict the existing formulation approaches to BRPs.

2.1. Objective functions in BRPs

User satisfaction has been commonly considered as the primary objective in BRPs. It is mainly measured by the number of due date violations (e.g., Brinkmann et al., 2015), unsatisfied demand including both docks and bikes (e.g., Contardo et al., 2012), penalty costs (e.g., Ho and Szeto, 2014), and so on. Repositioning costs are also considered in most studies, such as travel costs including travel time or distance (e.g., Benchimol et al., 2011; Angeloudis et al., 2014; Dell'Amico et al., 2014, 2016; Cruz et al., 2017), maximum tour distance (e.g., Schuijbroek et al., 2017), total travel and handling costs (e.g., Erdoğan et al., 2014), total redistribution cost (e.g., Nair et al., 2013), and total relocation and lost user costs (e.g., Caggiani and Ottomanelli, 2012). Besides single objective optimization, some studies considered the weighted sum of various measures, including the cost of unsatisfied demand and the coefficient of variations of the duration of all routes (e.g, Alvarez-Valdes et al., 2016), the total absolute deviation from the target number of bikes, the total number of loading/unloading quantities, and the overall time required for all routes (e.g., Di Gaspero et al., 2013, 2016; Raidl et al., 2013; Rainer-Harbach et al., 2013, 2015), total travel time and penalty cost (e.g., Ho and Szeto, 2017), total vehicle travel cost and the expected user dissatisfaction in the system (e.g., Zhang et al., 2017), the total number of unsatisfied customers and the vehicle's total operational time (e.g., Szeto et al., 2016), and travel, imbalance, substitution, and occupancy costs (e.g., Li et al., 2016). However, existing objectives have rarely considered environmental objectives. Indeed, repositioning operations are commonly carried out by fossil-fueled vehicles, which emit pollutants and greenhouse gases. These emissions can damage the environmental creditability of BSSs (Wiersma, 2010). It is therefore important to capture environmental objectives in BRPs. To the best of our knowledge, Shui and Szeto (2018) were the pioneers to capture an environmental objective in

BRPs. They minimized the weighted sum of total unmet demand and the fuel and CO_2 emission cost of the operating vehicle as the objective of their study.

One may argue that using bike-trailers for bike repositioning (e.g., Citibike in New York City) are ideal for mitigating CO_2 emissions during the operation. Bike-trailers can carry 3–5 bikes at most at one time (e.g., O'Mahony and Shmoys, 2015; Ghosh and Varakantham, 2017). They are suitable for the case where stations are close to each other, the BSS is in high usage, and traffic is at its peak (O'Mahony and Shmoys, 2015). However, since static repositioning usually happens during nighttime, the system usage and congestion impact can be ignored. In addition, to redistribute bikes for the demand in the next morning, the capacity of bike trailers is far from enough, which makes the bike repositioning inefficient. Furthermore, the route length can be far beyond the capability of the staff on bikes with trailers. It is unavoidable to use trucks to perform bike repositioning for an even medium size BSS.

2.2. Fuel consumption and CO_2 emission modeling

Other than BRPs, environmental issues have been considered in many transport studies, including those about vehicle routing problems. Emissions can be reduced by optimizing vehicle routes. In vehicle routing problems that consider environmental objectives (called green vehicle routing problems), CO_2 emissions or an approximate measure – fuel consumption – is usually considered as the model objective (e.g., Demir et al., 2012; Koç et al. 2014; Zhang et al., 2014; Ehmke et al., 2016; Xiao and Konak, 2016). Different CO_2 emission or fuel consumption models have been used in green vehicle routing problems. The measurable factors adopted in most of these models mainly include vehicle speed, acceleration or deceleration, gradient, and the weight of vehicle loads for certain types of vehicle and fuel (Scott et al., 2010; Demir et al., 2011; Suzuki, 2011; Lin et al., 2014; Zhang et al., 2015; Hosseini-Nasab and Lotfalian, 2017). For static bike repositioning, which usually happens in urban cities during the nighttime, the speed can be treated as constant because the congestion and vehicle flow impacts on the speed are very minor. The road gradient can be reflected in the asymmetric distances between two nodes. In addition, emissions during waiting time can be omitted when a perfect balance is considered because they are proportional to loading and unloading quantities and are constant in the objective function. Therefore, as indicated in the study of Xiao et al. (2012), the fuel consumption rate can be treated as linear with respect to vehicle loads when having the previous assumptions in static bike repositioning.

Xiao et al. (2012) also presented a fuel consumption model in detail, which is composed of the empty-load fuel consumption rate ρ_0, the full-load fuel consumption rate ρ^*, and the vehicle capacity Q_0. The full equation is given below:

$$\rho(q) = \rho_0 + \frac{\rho^* - \rho_0}{Q_0} * q \tag{1}$$

where q is the load on the vehicle. When the vehicle is empty, the vehicle has a fixed fuel consumption rate ρ_0, which relates to the vehicle type and the fuel type. The term $\frac{\rho^* - \rho_0}{Q_0}$ determines the quantity of fuel consumption induced by one unit increase in the vehicle load. Therefore, the total fuel consumption per unit of distance is the sum of fixed consumption and additional load consumption. On the basis of Eq. (1), Zhang et al. (2014) developed a CO_2 emission model, converting the fuel consumption into emissions through a conversion rate:

$$e(q) = CER * \left(\rho_0 + \frac{\rho^* - \rho_0}{Q_0} * q\right) * d \tag{2}$$

where CER is the CO_2 emission rate and d is the travel distance with a load q.

A similar model has also been proposed in the study of Kopfer et al. (2014), where the CO_2 emissions are proportional to the fuel consumption. Thus, the minimization of CO_2 emissions and fuel consumption are equivalent. In their study, the following is adopted as the objective function:

$$F(q) = a * d + b * q * d \tag{3}$$

where a denotes the fuel consumption per unit of distance and b denotes the fuel consumption per unit of payload and distance.

2.3. Broken bikes in BRPs

Other than environmental objectives, another important consideration in BSSs is broken bikes. It is almost unavoidable to have broken bikes in BSSs, due to careless use or accidents. The presence of broken bikes implies a waste of resources, as broken bikes take up the limited lockers in a station and are unusable (Kaspi et al., 2017). The numerical results of Kaspi et al. (2017) indicate that even a small fraction of unusable bikes can have a significant effect on user dissatisfaction. Therefore, the broken bikes need to be taken away from stations for repairs, which certainly consumes parts of the repositioning resources that are intentionally assigned to usable bikes. Therefore, when planning the repositioning works, broken bikes need to be considered together with usable bikes. However, most of the existing studies do not consider broken bikes. An exception is the study by Alvarez-Valdes et al. (2016) who studied bike repositioning with broken bikes, in which the vehicles transshipped usable bikes among stations, collected broken bikes at stations along the tours, and dropped the broken bikes off at the depot. Nevertheless, Alvarez-Valdes et al. (2016) did not consider vehicle emissions due to the repositioning.

Table 2.1
Summary of the characteristics of bike repositioning problems.

	Assumptions				Objective function							
References	No. of vehicles	MV	BB	Scenario	Dev	UD	DS	TT/ TD/ TC	CVD	PC	LQ/ HC	EI
Benchimol et al. (2011)	Single			Static				✓				
Contardo et al. (2012)	Multiple	✓		Dynamic		✓						
Chemla et al. (2013)	Single	✓		Static				✓				
Di Gaspero et al. (2013)	Multiple			Static	✓			✓			✓	
Angeloudis et al. (2014)	Multiple			Static				✓				
Erdoğan et al. (2014)	Single			Static				✓			✓	
Ho and Szeto (2014)	Single			Static						✓		
Rainer-Harbach et al. (2015)	Multiple	✓		Static	✓			✓			✓	
Alvarez-Valdes et al. (2016)	Multiple	✓	✓	Static				✓	✓			
Dell'Amico et al. (2016)	Multiple			Static				✓				
Li et al. (2016)	Single			Static				✓		✓		
Szeto et al. (2016)	Single			Static		✓		✓				
Cruz et al. (2017)	Single	✓		Static				✓				
Ho and Szeto (2017)	Multiple			Static				✓		✓		
Zhang et al. (2017)	Multiple			Dynamic			✓	✓				
Shui and Szeto (2018)	Single	✓		Dynamic		✓						✓
Szeto and Shui (2018)	Multiple			Static		✓		✓			✓	
This study	Multiple	✓	✓	Static								✓

MV: multiple visits; BB: broken bikes; Dev: deviation from the target number of bikes; UD: total unmet demand; DS: user dissatisfaction; TT: total travel time; TD: total travel distance; TC: total travel cost; CVD: coefficient of variation of the duration of all routes; PC: penalty cost; LQ: the total number of loading/unloading quantities; HC: handling cost; EI: environmental issues.

2.4. Modeling assumptions in BRPs

Existing BRPs, including those aforementioned, can be classified into different categories according to the characteristics of the target BSS and the availability of repositioning resources. In these problems, there could be more than one vehicle carrying out the repositioning work (e.g., Raviv et al., 2013; Alvarez-Valdes et al., 2016; Ho and Szeto, 2017). However, under some circumstances, a single vehicle could also handle the job (e.g., Benchimol et al., 2011; Chemla et al., 2013; Erdoğan et al., 2014). Some problems limited to at most a single visit of a vehicle to each station (e.g., Ho and Szeto, 2014; Szeto et al., 2016) while others considered multiple visits to stations (e.g., Chemla et al., 2013; Papazek et al., 2014; Rainer-Harbach et al., 2013, 2015). In fact, multiple visits to a station are required when the capacity of a single vehicle is insufficient to deal with the demand at that station. As demonstrated in the numerical studies of this paper, multiple visits can also reduce vehicle emissions.

Some of the studies discussed before are summarized in Table 2.1. Compared with other static bike repositioning studies, this study simultaneously considers broken bikes, an environmental objective, and multiple visits to depots/stations.

2.5. Formulation approaches

To formulate BRPs, various approaches can be used. Raviv et al. (2013) presented three different MILP models in their study, including an Arc-Indexed (AI) Formulation, a Time-Indexed (TI) Formulation, and a Sequence-Indexed (SI) Formulation. The AI formulation is the most popular in BRPs and uses binary variables to indicate the consecutive visits of two nodes. Thus, the routing decision variables relate to two nodes, implying an arc in a route. The TI formulation adds a time index to the decision variables, so it can handle multiple periods in the planning horizon and broadens the feasible region compared to the AI formulation. Unlike the former two formulations focusing on arcs, the SI formulation pairs a station with its order in the visit sequence. Therefore, only one node index appears in the decision variables, which makes it capable of tackling multiple visit instances. The TI formulation can adapt to almost all situations as well as dynamic planning because of the time index introduced while the AI formulation cannot. Multiple visits to stations and transshipments can both be allowed in the TI formulation. However, time discretization might cause the loss of accuracy and also increase the problem complexity significantly compared with the AI formulation, especially when the problem can be modeled using the AI formulation. The SI formulation is not as flexible as the TI formulation but outperforms the AI formulation with more tolerances for assumptions. However, the SI formulation receives the least attention in the literature.

2.6. Summary

It is important to capture environmental objectives in BRPs. Moreover, when the vehicle speed is constant, the fuel consumption rate is linear with respect to vehicle loads as shown in Eq. (1). Thus, for a certain type of fuel, the CO_2 emissions are the product of the fuel-to-CO_2 conversion rate, total travel distance, and fuel consumption rate, as shown in Eq. (2), which is equivalent to Eq. (3). Furthermore, broken bikes can be treated as another type of bike and should be tackled simultaneously. In addition, multiple visits may be necessary for bike repositioning. To model this, the SI formulation can be used and solved by commercial solvers.

3. Model formulation

Consider a BSS consisting of the depot and stations. These stations can be classified into three types: pick-up, drop-off, and balanced. A pick-up station has a higher initial inventory of usable bikes than the target inventory. A drop-off station has a higher target inventory of usable bikes than the initial inventory. A balanced station has the initial inventory equal to the target inventory. Multiple homogenous vehicles with fixed capacity depart from the depot (denoted by 0) nonempty, transship usable bikes among stations to meet the target inventory level of each station, take all broken bikes from stations to the depot for repairs, and transport redundant usable bikes back to the depot. We set the monotonicity constraint for the loading/unloading instructions. That is to say, bikes cannot be dropped off at a "pick-up station" during the repositioning process and bikes cannot be loaded from a "drop-off station" during the repositioning process. All stations and the depot can be visited multiple times. The target inventory level of each station must be met. All bikes on each vehicle should be unloaded to the depot at the end of the tour. In addition, once broken bikes are loaded onto the vehicles, they cannot be dropped off at any other stations except for the depot. Balanced stations with zero broken bikes do not need to be visited. The depot is supposed to have infinite bike stocks and infinite capacity. The total CO_2 emissions of all vehicles are used to assess the performance of the repositioning operation. We assume that the CO_2 emissions are only produced when a vehicle is moving and we ignore the emissions during waiting. Moreover, the amount of emissions just relates to the load and travel distance of the vehicles. The objective is to reduce the total emissions.

3.1. Notations

Sets

S	The set of stations
S_0	The set of nodes, including the stations and the depot
V	The set of vehicles

Parameters

p_i	The initial inventory of usable bikes at station $i \in S$
q_i	The target inventory of usable bikes at station $i \in S$
b_i	The quantity of broken bikes at station $i \in S$
d_{ij}	Travel distance from node $i \in S_0$ to node $j \in S_0$
ρ_0	The empty-load fuel consumption rate of each vehicle (liters/km)
ρ^*	The full-load fuel consumption rate of each vehicle (liters/km)
CER	The CO_2 emission rate (kg/liter)
Q_k	The capacity of vehicle k
A	An upper bound on the number of stops of each vehicle
M	A large number for linearizing the objective function

Decision variables

x_{iak}	$=\begin{cases}1, \text{ if node } i \text{ is the } a^{\text{th}} \text{ stop of vehicle } k \\ 0, \text{ otherwise}\end{cases}$
y^G_{iak}	The number of usable bikes loaded onto or unloaded from vehicle k at node i at its a^{th} stop, an integer variable (a positive number implies that a loading operation occurs there)
y^B_{iak}	The number of broken bikes loaded onto or unloaded from vehicle k at node i at its a^{th} stop, an integer variable

Auxiliary variables

y^G_{ak}	The number of usable bikes on vehicle k after loading/unloading at its a^{th} stop, a nonnegative integer variable
y^B_{ak}	The number of broken bikes on vehicle k after loading/unloading at its a^{th} stop, a nonnegative integer variable
z_{aijk}	The emissions produced when vehicle k travels from node i and arrives at node j at its a^{th} stop

3.2. Sequence-indexed formulation

The problem can be mathematically stated as follows:

$$\text{Minimize} \quad \sum_{k\in V}\sum_{a=2}^{A}\sum_{i\in S_0}\sum_{j\in S_0, i\neq j} z_{aijk} \tag{4}$$

Subject to

$$\sum_{i\in S_0} x_{iak} = 1 \quad \forall\, a = 1, \cdots, A, \quad \forall\, k \in V \tag{5}$$

$$x_{01k} = 1, \quad \forall\, k \in V \tag{6}$$

$$x_{0Ak} = 1, \quad \forall\, k \in V \tag{7}$$

$$x_{0ak} + x_{0,a+1,k} - x_{0,a+2,k} \leq 1, \quad \forall\, a = 1, \cdots, A-2, \quad \forall\, k \in V \tag{8}$$

$$x_{iak} + x_{i,a+1,k} \leq 1, \quad \forall\, i \in S, a = 2, \cdots, A-1, \quad \forall\, k \in V \tag{9}$$

$$p_i - \sum_{k\in V}\sum_{a=1}^{A} y_{iak}^{G} = q_i, \quad \forall\, i \in S \tag{10}$$

$$b_i - \sum_{k\in V}\sum_{a=1}^{A} y_{iak}^{B} = 0, \quad \forall\, i \in S \tag{11}$$

$$-Q_k \cdot x_{iak} \leq y_{iak}^{G} \leq Q_k \cdot x_{iak}, \quad \forall\, i \in S_0, a = 1, \cdots, A, \quad \forall\, k \in V \tag{12}$$

$$0 \leq y_{iak}^{B} \leq b_i \cdot x_{iak}, \quad \forall\, i \in S, a = 1, \cdots, A, \quad \forall\, k \in V \tag{13}$$

$$-Q_k \cdot x_{0ak} \leq y_{0ak}^{B} \leq 0, \quad \forall\, a = 1, \cdots, A, \quad \forall\, k \in V \tag{14}$$

$$\min(0, p_i - q_i) \leq y_{iak}^{G} \leq \max(0, p_i - q_i), \quad \forall\, i \in S, a = 2, \cdots, A-1, \quad \forall\, k \in V \tag{15}$$

$$y_{ak}^{G} = y_{a-1,k}^{G} + \sum_{i\in S_0} y_{iak}^{G}, \quad \forall\, a = 2, \cdots, A, \quad \forall\, k \in V \tag{16}$$

$$y_{ak}^{B} = y_{a-1,k}^{B} + \sum_{i\in S_0} y_{iak}^{B}, \quad \forall\, a = 2, \cdots, A, \quad \forall\, k \in V \tag{17}$$

$$y_{1k}^{G} = y_{01k}^{G}, \quad \forall\, k \in V \tag{18}$$

$$y_{1k}^{B} = 0, \quad \forall\, k \in V \tag{19}$$

$$y_{Ak}^{G} = 0, \quad \forall\, k \in V \tag{20}$$

$$y_{Ak}^{B} = 0, \quad \forall\, k \in V \tag{21}$$

$$y_{ak}^{G} + y_{ak}^{B} \leq Q_k, \quad \forall\, a = 1, \cdots, A, \quad \forall\, k \in V \tag{22}$$

$$CER \cdot \left[\rho_0 + \frac{\rho^* - \rho_0}{Q} \cdot (y_{a-1,k}^{G} + y_{a-1,k}^{B})\right] \cdot d_{ij} - z_{aijk} \leq M \cdot [2 - (x_{i,a-1,k} + x_{jak})], \quad \forall\, i, j \in S_0, a = 2, \cdots, A, \quad \forall\, k \in V \tag{23}$$

$$x_{iak} \in \{0, 1\}, \quad \forall\, i \in S_0, a = 1, \cdots, A, \quad \forall\, k \in V \tag{24}$$

$$y_{iak}^{G}, \quad \text{integers}, \quad \forall\, i \in S_0, a = 1, \cdots, A, \quad \forall\, k \in V \tag{25}$$

$$y_{iak}^{B}, \quad \text{integers}, \quad \forall\, i \in S_0, a = 1, \cdots, A, \quad \forall\, k \in V \tag{26}$$

$$y_{ak}^{G} \geq 0, \quad \text{integers}, \quad \forall\, a = 1, \cdots, A, \quad \forall\, k \in V \tag{27}$$

$$y_{ak}^{B} \geq 0, \quad \text{integers}, \quad \forall\, a = 1, \cdots, A, \quad \forall\, k \in V \tag{28}$$

$$z_{aijk} \geq 0, \quad \forall\, i, j \in S_0, a = 2, \cdots, A, \quad \forall\, k \in V \tag{29}$$

The objective (4) is to minimize the total CO_2 emissions of all the vehicles. Constraints (5) guarantee that each vehicle visits one station at one time. Constraints (6) and (7) restrict the tour of each vehicle to start from and end at the depot, respectively. Constraints (8) make sure that no vehicle has two consecutive stops at the depot, except possibly the last stop, after all loading/unloading activities are completed (Raviv et al., 2013). Constraints (9) prevent the situation when a vehicle visits a station at two consecutive stops. Constraints (10) stipulate the perfect balance condition held at each station at the end of the repositioning operation, i.e., after the repositioning is finished, the inventory level of usable bikes at each station equals the corresponding target inventory level. Note

that the second term on the left-hand side is the sum of loading/unloading quantities at all stops of all vehicles at station i. Constraints (11) imply that all broken bikes are transported away from all stations before the end of repositioning operation. Constraints (12)–(14) indicate that there are no loading/unloading activities for any bike at a certain station if this station is not visited by any vehicle. Constraints (15) set the upper and lower bounds of loading/unloading quantities of usable bikes of each vehicle at each stop. Constraints (16) and (17) define the numbers of usable bikes and broken bikes on each vehicle after leaving the a^{th} stop, respectively. Constraints (18) imply that the number of usable bikes on each vehicle after leaving the first stop is the loading quantity at the depot. Constraints (19) mean that there are no broken bikes on each vehicle after leaving the first stop. Constraints (20) and (21) require that all types of carried bikes should be unloaded from each vehicle at the end of its tour. Constraints (22) are the vehicle capacity constraints. Constraints (23) define the emissions produced when vehicle k travels from node i and arrives at node j at its a^{th} stop. Constraints (24)–(29) are the domain constraints.

Constraints (15) can be linearized by introducing an auxiliary binary variable σ_i and extra constraints (30)–(33):

$$-\sigma_i \cdot M \le p_i - q_i, \quad \forall\, i \in S \tag{30}$$

$$-\sigma_i \cdot M \le y^G_{iak} \le p_i - q_i + \sigma_i \cdot M, \quad \forall\, i \in S, \quad \forall\, k \in V \tag{31}$$

$$p_i - q_i \le (1-\sigma_i)\cdot M, \quad \forall\, i \in S \tag{32}$$

$$p_i - q_i - (1-\sigma_i)\cdot M \le y^G_{iak} \le (1-\sigma_i)\cdot M, \quad \forall\, i \in S, \quad \forall\, k \in V \tag{33}$$

In general, a higher value of the upper bound on the number of stops of each vehicle (A) is supposed to provide better solutions. However, the higher value leads to more decision variables as well as a longer running time. Therefore, we can first compute the lower bound A_l for the value of A, and then increase A from the lower bound until the objective value cannot be improved. This lower bound consists of three parts as stated below.

Firstly, all the stations with broken bikes or insufficient/excess usable bikes must be visited at least once and the depot must be visited at the start and the end of the tour (twice). Define a new set $S_U = \{i | i \in S,\ p_i \ne q_i \ \text{ or } \ b_i \ne 0\}$ that contains all these stations. Then the number of stops should be no less than $|S_U| + 2$.

Secondly, if the sum of demand/supply of all the stations exceeds the vehicle capacity Q, the depot needs to be visited halfway. Let n_d be the number of additional visits to the depot (except the first and last stops of each vehicle). Then it can be expressed as

$$n_d = \begin{cases} \left\lfloor \frac{\sum_{i\in S}(p_i - q_i) + \sum_{i\in S} b_i}{Q} \right\rfloor, & \text{if} \quad \sum_{i\in S}(p_i - q_i) \geqslant 0 \\ \max\left(\left\lfloor \frac{\sum_{i\in S}(q_i - p_i)}{Q} \right\rfloor, \left\lfloor \frac{\sum_{i\in S} b_i}{Q} \right\rfloor \right), & \text{otherwise} \end{cases} \tag{34}$$

Lastly, if the demand of a specific station exceeds Q, this station must be visited multiple times. Define two new sets $S_A^+ = \{i | i \in S,\ p_i - q_i > 0 \ \ \& \ \ p_i - q_i + b_i > Q\}$ and $S_A^- = \{i | i \in S,\ p_i - q_i < 0 \ \ \& \ \ \max(q_i - p_i,\ b_i) > Q\}$, which contain all the stations that have total loading/unloading quantities larger than the vehicle capacity. Let $n_{S_A^+}$ and $n_{S_A^-}$ be the numbers of additional visits to the stations in the corresponding sets. Then,

$$n_{S_A^+} = \sum\nolimits_{i\in S_A^+} \left\lfloor \frac{p_i - q_i + b_i}{Q} \right\rfloor \text{ and} \tag{35}$$

$$n_{S_A^-} = \sum\nolimits_{i\in S_A^-} \left\lfloor \frac{\max(q_i - p_i,\ b_i)}{Q} \right\rfloor \tag{36}$$

Therefore, the lower bound for the value of A can be computed as

$$A_l = |S_U| + 2 + n_d + n_{S_A^+} + n_{S_A^-} \tag{37}$$

To balance the solution equality and running time, in our experiments, the start value of A is set as A_l. Then A increases until the objective value cannot be improved.

4. Numerical studies

We will first discuss the effects of different factors on the repositioning operation strategy and the CO_2 emissions in Sections 4.1–4.5, including:

1. The effect of demand tolerance (the acceptable deviation to the target demand)
2. The effect of the percentage of broken bikes in the network
3. The effect of link distances between stations
4. The effect of multiple visits
5. The effect of vehicle capacity

Then we will compare the solutions obtained from emission minimization and total travel distance minimization in Section 4.6.

Table 4.1
Parameter settings of the CO_2 emission model for all numerical experiments.

Settings	Value
CO_2 emission rate in terms of diesel oil *CER* (kg/liter)	2.61
The empty-load fuel consumption rate ρ_0 (liters/km)	0.296
The full-load fuel consumption rate ρ^* (liters/km)	0.39

Finally, we will show the performance of the model and solution methods used in Section 4.7.

For these purposes, we set different instances and formed an MILP for each scenario. We only used ILOG CPLEX 12.6 invoked by a C++ program in Visual Studio 2010 to solve the model for each scenario, except that for a large network instance with 90 stations, a clustering method based on the nearest neighbor heuristic was used before executing the optimization program. This program was executed on a computer with an Intel® Core™ i7-4790 CPU and 32 GB of RAM. For all scenarios investigating the effects of different factors in Sections 4.1–4.5, there are 6 stations and one depot. In Sections 4.6 and 4.7, the benchmark instances created by Rainer-Harbach et al. (2015) based on Citybike Vienna are used. In all numerical experiments in Section 4, unless otherwise specified, there is only one vehicle and its capacity is 20 bikes. The parameters in the CO_2 emission model (2) for all numerical experiments are listed in Table 4.1 and follow the values in Ubeda et al. (2011).

A base scenario is set for the comparison between different settings in Sections 4.1–4.5. The information of the stations in the base scenario is displayed in Table 4.2. Both the "initial inventory" and "target inventory" refer to usable bikes in the following contents. The travel distances between nodes are shown in Table 4.3. For this base scenario, the optimal solution is shown in Table 4.4.

The first row in Table 4.4 is the visit sequence of the vehicle to each node. Each number in this row is the node number and 0 represents the depot. It can be seen that the first and last stops of the vehicle are both the depot and the depot is visited at the 7th stop. Moreover, it is observed that Station 2 is visited twice because its demand (25 usable bikes) exceeds the capacity of the vehicle (20 bikes). The second row shows the number of usable bikes loaded onto or unloaded from the vehicle. A positive number means loading that number of bikes onto the vehicle whereas a negative number means unloading bikes from the vehicle and the unloading quantity equals the absolute value of that number. According to the second row, the depot is visited at the 7th stop to collect extra 9 usable bikes for the following stations. The third row shows the number of broken bikes loaded onto or unloaded from the vehicle at each stop. When the vehicle comes back to the depot halfway, it unloads all the broken bikes to the depot to make room for the usable bikes to load onto the vehicle. The last row displays the total number of bikes on the vehicle after leaving the corresponding stop. The total CO_2 emissions in this scenario are 5.824 kg.

4.1. The effect of demand tolerance

This section will discuss the effect of demand tolerance on the CO_2 emissions. Under the perfect balance condition, all station demands must be satisfied, which means that the final inventory level of usable bikes of each station must be equal to its target inventory. If a tolerance δ_i is assigned to the demand of a station$i$, the final inventory of usable bikes at that station should be controlled within the range $[q_i - \delta_i, q_i + \delta_i]$ and the range between zero and its station capacity, where $\delta_i = q_i P$ and P is the percentage of demand tolerance. In this section, 7 scenarios with different values of P will be studied: P = 0%, 5%, …, 30%.

Table 4.5 shows the optimal route and the corresponding vehicle loads, number of stops, and CO_2 emissions under different percentages of demand tolerance. The perfect balance scenario is the base scenario mentioned earlier. When $P = 5\%$, the optimal route does not change compared with the perfect balance scenario. The initial load on the vehicle slightly decreases from 10 bikes to 9 bikes. Thus, there is nearly no difference between the emissions under these two scenarios. When $P = 10\%$, the first four stops in the optimal route stay the same but the following visit sequence changes greatly compared with the former scenario. Station 2 is still visited twice, but the depot is not visited halfway during the tour, i.e., it is visited just at the start and the end of the tour. This result indicates that the vehicle does not need to collect extra usable bikes or unload bikes at the depot halfway. Therefore, the vehicle is full-loaded at the start of the tour. In addition, the route has one stop less than the former case and the emissions decrease from 5.812 kg to 5.472 kg. When $P = 15\%$, Station 4 is visited two stops earlier compared with the 10% case. The emissions are further reduced to 5.205 kg. When $P = 20\%$, Station 2 is only visited once and the tour length is reduced to 8 stops. The emissions are 4.848 kg. In the cases of the 25% and 30% tolerance, the optimal route remains the same as that in the case of the 20% tolerance, but the emissions keep decreasing as the percentage of demand tolerance increases. The trend of emissions under different percentages of demand tolerance is displayed in Fig. 4.1. In general, when the percentage of demand tolerance increases, the CO_2 emissions

Table 4.2
Station information in the base scenario.

Station	1	2	3	4	5	6	Total
Station capacity	20	25	17	20	25	15	122
Initial inventory	5	0	17	15	22	7	66
Target inventory	18	25	5	18	15	4	85
Broken bikes	3	4	0	3	1	2	13

Table 4.3
Travel distances (in hundred meters) between stations in the base scenario.

	Depot	1	2	3	4	5	6
Depot	0	14	10	15	15	16	12
1	11	0	7	9	4	12	6
2	12	13	0	10	12	8	4
3	14	10	6	0	8	6	14
4	7	10	8	13	0	11	6
5	6	16	14	10	7	0	6
6	16	9	14	6	13	8	0

Table 4.4
Optimal repositioning route and loading instructions in the base scenario.

Node	0	2	6	3	2	5	0	1	4	0	
Loading instruction for usable bikes	10	−10	3	12	−15	7	9	−13	−3	0	Emissions = 5.824 kg
Loading instruction for broken bikes	0	0	2	0	4	1	−7	3	3	−6	
Vehicle load	10	0	5	17	6	14	16	6	6	0	

Table 4.5
The optimal solutions under different percentages of demand tolerance.

		Optimal route	Loads on the vehicle	Number of stops	Emissions (kg)
Perfect balance		0-2-6-3-2-5-0-1-4-0	10-0-5-17-6-14-16-6-6-0	10	5.824
Percentage of demand tolerance	5%	0-2-6-3-2-5-0-1-4-0	9-0-5-17-6-14-16-6-6-0	10	5.812
	10%	0-2-6-3-1-2-5-4-0	20-0-5-17-8-9-16-15-0	9	5.472
	15%	0-2-6-3-1-4-2-5-0	20-0-5-17-8-10-12-18-0	9	5.205
	20%	0-2-6-3-1-4-5-0	20-4-9-20-9-12-17-0	8	4.848
	25%	0-2-6-3-1-4-5-0	19-4-8-19-9-12-17-0	8	4.816
	30%	0-2-6-3-1-4-5-0	18-4-8-19-9-12-16-0	8	4.796

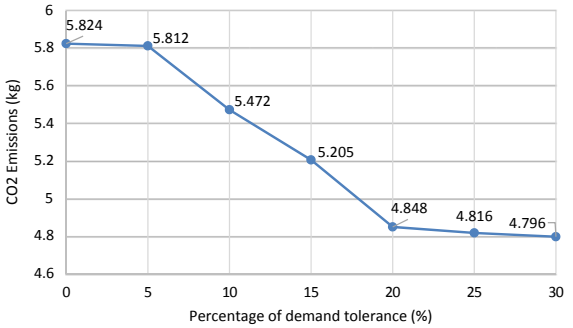

Fig. 4.1. The CO_2 emissions under different percentages of demand tolerance.

Table 4.6
The ranges of the final inventory level for each station under different demand tolerances.

		Station					
		1	2	3	4	5	6
Target inventory level		18	25	5	18	15	4
Demand tolerances	0	18	25	5	18	15	4
	5%	18	[24,25]	5	18	15	4
	10%	[17,19]	[23,25]	5	[17,19]	[14,16]	4
	15%	[16,20](17)	[22,25]	5	[16,20]	[13,17]	4
	20%	[15,20](19)	[20,25]	[4,6]	[15,20]	[12,18]	4
	25%	[14,20](18)	[19,25]	[4,6]	[14,20](15)	[12,18]	[3,5]
	30%	[13,20](18)	[18,25]	[4,6]	[13,20](15)	[11,19]	[3,5]

Table 4.7
The optimal routes, loading instructions for usable bikes, and loads of usable bikes on the vehicle under different demand tolerances.

Tolerance		Results
15%	Optimal route	0-2-6-3-1-4-2-5-0
	Loading instructions for usable bikes	(20)-(-20)-(3)-(12)-(-12)-(-1)-(-2)-(5)-(-5)
	Loads of usable bikes on the vehicle	20-0-3-15-3-2-0-5-0
	Loading instructions for broken bikes	(0)-(0)-(2)-(0)-(3)-(3)-(4)-(1)-(-13)
20%	Optimal route	0-2-6-3-1-4-5-0
	Loading instructions for usable bikes	(20)-(-20)-(3)-(11)-(-14)-(0)-(4)-(-4)
	Loads of usable bikes on the vehicle	20-0-3-14-0-0-4-0
	Loading instructions for broken bikes	(0)-(4)-(2)-(0)-(3)-(3)-(1)-(-13)
25%	Optimal route	0-2-6-3-1-4-5-0
	Loading instructions for usable bikes	(19)-(-19)-(2)-(11)-(-13)-(0)-(4)-(-4)
	Loads of usable bikes on the vehicle	19-0-2-13-0-0-4-0
	Loading instructions for broken bikes	(0)-(4)-(2)-(0)-(3)-(3)-(1)-(-13)
30%	Optimal route	0-2-6-3-1-4-5-0
	Loading instructions for usable bikes	(18)-(-18)-(2)-(11)-(-13)-(0)-(3)-(-3)
	Loads of usable bikes on the vehicle	18-0-2-13-0-0-3-0
	Loading instructions for broken bikes	(0)-(4)-(2)-(0)-(3)-(3)-(1)-(-13)

decrease.

Table 4.6 summarizes the ranges of the final inventory level for each station under different demand tolerances. The lower and upper bounds are rounded up to the nearest integer. If the final inventory level hits the upper or lower bound in the range, the corresponding number is underlined. If not, the final inventory level is recorded in the parenthesis after the range.

For Station 2, its initial inventory level is 0 usable bike and the target inventory level is 25 usable bikes. When the demand tolerance increases, the lower bound of the final inventory keeps decreasing, but the upper bound stays the same (25 usable bikes) because the station capacity is 25 bikes. The final inventory levels always hit the corresponding lower bound in all scenarios, because Station 2 is in need of usable bikes and a lower final inventory level implies lower demand, leading to smaller loads on the vehicle and vehicle emissions.

For Station 3, Station 5, and Station 6, they have extra usable bikes that need to be transported away. The final inventories at these stations always hit the corresponding upper bound in all scenarios, because collecting fewer bikes can also make the loads on the vehicle and hence vehicle emissions smaller.

For Station 1 and Station 4, they are in need of usable bikes. However, unlike station 2, which is also a drop-off station, their final inventory levels are not always equal to the lower bound of the corresponding range and are in fact higher than the lower bound. In the case of the 15% tolerance, Station 1 is visited before Station 4 and the second visit to Station 2. Extra usable bikes are dropped off at Station 1, because (1) these bikes obtained from the previous pickup stations have to unload at some drop-off stations anyway and (2) when they are dropped off earlier, fewer bikes are on the vehicle for the later part of the route, leading to lower vehicle emissions. For the cases of the 20%, 25%, and 30% tolerance, since the final inventory range of Station 1's succeeding station (Station 4) contains the initial inventory level (15 usable bikes), no extra usable bikes are needed for Station 4 (see Table 4.7 for reference). In addition, the two preceding pick-up stations (Station 3 and Station 6) of Station 1 already have their initial inventories more than their corresponding upper bound, and therefore at least the difference between them has to be picked up by the vehicle and should be dropped off as soon as possible. As a result, the final inventory at Station 1 is larger than its lower bound in each of these scenarios.

In summary, when a tolerance to the demands of stations increases, the CO_2 emissions decrease, and the route, vehicle load, or loading instructions may be adjusted to reduce the emissions. Moreover, the number of stops in an optimal route is non-increasing with respect to the tolerance. Furthermore, both the upper and lower bounds of the final inventory may not be the resulting inventory level when a demand tolerance is allowed.

4.2. The effect of the percentage of broken bikes

In this section, we still consider 79 bikes as in Table 4.2. The initial total number of bikes in each station is also the same as that in Table 4.2. However, we varied the percentage of broken bikes. The percentage of broken bikes increased from 0 to 20% of the total number of bikes at regular intervals equal to 5%. When 5% of total bikes were broken, the total number of broken bikes was 3.95, which was rounded up to the nearest integer (i.e., 4) and then distributed evenly among four stations (without loss of generality, we picked Stations 1, 3, 4, 5). To eliminate the effect of the spatial distribution of broken bikes on the emissions, the stations without broken bikes in the "5%" scenario also had no broken bikes in all other scenarios. The initial inventory (of usable bikes) at each station was then constructed using the total number of bikes minus the corresponding number of broken bikes. Other station information, including the station capacity and the target inventory of usable bikes, are the same as those in Table 4.2. The broken bike distributions under different percentages are shown in Table 4.8. The travel distances between stations are the same as those in the base scenario shown in Table 4.3.

The results are displayed in Table 4.9. When there are no broken bikes, the optimal route has 8 stops and the depot is not visited

Table 4.8
Station information with different percentages of broken bikes.

Station		1	2	3	4	5	6	Total
Percentage of broken bikes	0%	0	0	0	0	0	0	0
	5%	1	0	1	1	1	0	4
	10%	2	0	2	2	2	0	8
	15%	3	0	3	3	3	0	12
	20%	4	0	4	4	4	0	16

Table 4.9
The optimal routes under different percentages of broken bikes.

		Optimal route	Loads on the vehicle	Number of stops	Emissions (kg)
Percentage of broken bikes	0	0-1-2-6-3-2-5-0	14-4-0-5-17-0-8-0	8	4.436
	5%	0-2-6-3-1-4-2-5-0	17-0-5-17-7-7-3-11-0	9	4.994
	10%	0-2-6-3-1-4-2-5-0	20-0-5-17-7-7-6-14-0	9	5.082
	15%	0-2-6-3-1-2-5-4-0	20-0-5-17-7-6-14-14-0	9	5.408
	20%	0-1-4-0-2-6-3-2-5-0	18-8-8-8-0-5-17-4-12-0	10	5.826

halfway during the journey. The CO_2 emissions are 4.436 kg. When the percentage of broken bikes increases to 5% and 10%, Station 4 needs to be visited because broken bikes can be found there. Therefore, the emissions increase in these two cases compared with the base case (0% broken bikes). When the percentage of broken bikes increases to 15%, the visit order of Station 4 in the optimal route changes and so do the vehicle loads. The emissions increase to 5.408 kg. For the case of 20% broken bikes, the optimal route changes greatly and the depot is visited halfway during the journey. The number of stops increases to 10 and the emissions increase to 5.826 kg. This increasing trend of emissions is displayed in Fig. 4.2.

In summary, when the percentage of broken bikes increases, the CO_2 emissions increase. The number of stops is a non-decreasing function of the percentage of broken bikes. The route and vehicle loads may be adjusted due to the change in the percentage.

4.3. The effects of distances between stations

This section will discuss the effects of the distance between two specific stations on the CO_2 emissions. To show different possibilities, we created four different scenarios as shown in Table 4.10. In each scenario, the distance of one link in the base scenario increased.

4.3.1. Scenarios 1 and 2

There is a base scenario for the comparison with Scenarios 1 and 2. The station information and travel distances in the base scenario for the comparison follow Tables 4.2 and 4.3, respectively. The optimal solution in this base scenario is shown in Table 4.4 and is also reported in the first row of Table 4.11.

Scenario 1: Double the distance between Station 2 and Station 6

Link 2-6 is in an optimal route in the base scenario. If the distance between Station 2 and Station 6 increases from 4 to 8, the optimal solution does not change. As shown in the row called "Double d_{26}" in Table 4.11, the optimal route is still 0-2-6-3-2-5-0-1-4-0 and link 2-6 is also in the optimal route. However, as the link distance doubles, the CO_2 emissions increase to 6.133 kg, which increases by 5.3% compared with the base scenario.

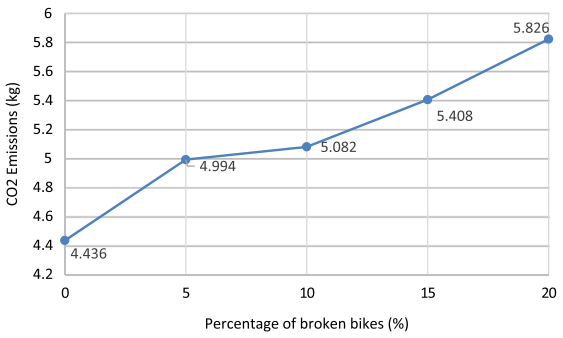

Fig. 4.2. The CO_2 emissions under different percentages of broken bikes.

Table 4.10
Four scenarios for studying the effect of link distance on emissions.

	The link is in an optimal route before the increase	The link is in an optimal route after the increase
Scenario 1	Yes	Yes
Scenario 2	No	No
Scenarios 3a and 3b	Yes	No

Table 4.11
The optimal routes and emissions in Scenarios 1 and 2 in Section 4.3.

	Optimal route	CO_2 emissions (kg)
Base scenario	0-2-6-3-2-5-0-1-4-0	5.824
Scenario 1: Double d_{26}	0-2-6-3-2-5-0-1-4-0	6.133
Scenario 2: Double d_{46}	0-2-6-3-2-5-0-1-4-0	5.824

Scenario 2: Double the distance between Station 4 and Station 6

Link 4-6 is not in an optimal route in the base scenario. If the distance between Station 4 and Station 6 increases from 6 to 12, the optimal route and emissions do not change and link 4-6 is still not in the optimal route as shown in the last row of Table 4.11.

4.3.2. Scenarios 3a and 3b

For Scenarios 3a and 3b, a symmetric network was created to demonstrate the two possibilities on emissions after a link distance on an optimal route increases. The station information and distance matrix for the base scenario are displayed in Tables 4.12 and 4.13, respectively. In this base scenario, the two optimal routes are 0-5-6-1-2-3-4-0 and 0-2-1-6-5-4-3-0. The CO_2 emissions are both 3.999 kg as shown in the "Base scenario" row of Table 4.14.

Scenario 3a: Double the distance between the depot and Station 5

The link between the depot and Station 5 is only in one optimal route. If the distance of this link increases from 7 to 14, the optimal solution will change. As shown in the "Double d_{05}" row of Table 4.14, the optimal route after this increase is 0-2-1-6-5-4-3-0 and Link 0-5 is not in an optimal route any more. Although the visit sequence of the vehicle changes compared with the base scenario, the CO_2 emissions stay the same as those in the base scenario. It is because in the base scenario, there are two optimal routes having the same emissions. Therefore, when the distance of one link in one of the two optimal routes but not both in the base scenario increases, the other optimal route is used after the increment and hence the emissions remain unchanged.

Scenario 3b: Double the distance between Station 1 and Station 6

The link between Stations 1 and 6 appears in both optimal routes in the base scenario. If the distance between these stations increases from 9 to 18, the two optimal solutions change to the one as shown in the last row of Table 4.14. Link 6-1 is not in an optimal route after the increment and the total emissions increase to 4.179 kg. Unlike Scenario 3a, the existence of two optimal routes cannot help to maintain the emission level because when the distance of Link 6-1 increases, the vehicle emissions of both routes increase. Unlike Scenario 1, the increase in distance is relatively large so that Link 6-1 is not in the resulting optimal route after the increase in distance.

4.3.3. Summary

In summary, the effects of distances between stations on emissions are shown in Table 4.15.

4.4. The effect of multiple visits

This section will explain the necessity of multiple visits. The vehicle has multiple visits to the depot and stations due to different

Table 4.12
Station information in the base scenario in Section 4.3.2.

Station	1	2	3	4	5	6	Total
Station capacity	20	25	17	20	25	15	122
Initial inventory	15	25	8	14	22	6	90
Target inventory	17	20	11	17	17	8	90
Broken bikes	2	0	3	3	0	2	10

Table 4.13
Travel distances (in hundred meters) between stations in Scenarios 3a and 3b in Section 4.3.2.

	Depot	1	2	3	4	5	6
Depot	0	8	7	7	7	7	7
1	8	0	5	13	15	13	9
2	7	5	0	9	12	14	12
3	7	13	9	0	4	12	14
4	7	15	12	4	0	9	13
5	7	13	14	12	9	0	6
6	7	9	12	14	13	6	0

Table 4.14
The optimal routes and emissions in Scenarios 3a and 3b in Section 4.3.2.

	Optimal route	Emissions (kg)
Base scenario	0-5-6-1-2-3-4-0 and 0-2-1-6-5-4-3-0	3.999
Scenario 3a: Double d_{05}	0-2-1-6-5-4-3-0	3.999
Scenario 3b: Double d_{16}	0-6-5-4-3-2-1-0	4.179

Table 4.15
The effects of distances between stations on the optimal routes and CO_2 emissions in different scenarios.

	The link is in an optimal route before the increase	The link is in an optimal route after the increase	Change of the optimal route	Change of CO_2 emissions
Scenario 1	Yes	Yes	No	Increase
Scenario 2	No	No	No	Unchanged
Scenario 3a	Yes	No	Yes	Unchanged
Scenario 3b	Yes	No	Yes	Increase

reasons: (1) insufficient vehicle capacity to cope with the total excess supply of all stations or the single excess demand of a specific station, (2) to decrease vehicle loads by dropping off broken bikes halfway, and (3) to satisfy the demands over several visits to reduce the vehicle loads. To illustrate them, different datasets from the base scenario are used in the following subsections.

4.4.1. Multiple visits due to excess supply or demands

When the absolute value of either the sum of the supply of all stations or the single demand of a specific station exceeds the vehicle capacity, the vehicle needs to visit the depot and/or a specific station multiple times. Two instances are provided for these two scenarios. They share the same distance matrix as shown in Table 4.16.

Scenario 1: Multiple visits to the depot

A new set of stations having information as shown in Table 4.17 is used to demonstrate the need of multiple-visit to the depot. It can be found that the total supply from all stations is 22 usable bikes, which means that 22 usable bikes need to be transported away from the stations to the depot. However, the vehicle capacity is only 20 bikes. Therefore, the depot is visited halfway to drop off some bikes. The optimal route in Scenario 1 is 0-3-2-5-0-1-4-0.

Scenario 2: Multiple visits to stations

A set of stations having different demands as shown in Table 4.18 is used to illustrate the need for multiple-visit to stations. The

Table 4.16
Travel distances (in hundred meters) between stations in the two scenarios in Section 4.4.1.

	Depot	1	2	3	4	5	6
Depot	0	13	15	15	19	13	9
1	12	0	8	17	8	13	9
2	12	20	0	16	18	15	20
3	17	19	6	0	12	12	19
4	10	8	7	19	0	17	5
5	7	12	9	17	13	0	11
6	9	10	10	6	12	20	0

Table 4.17
Station information in Scenario 1 in Section 4.4.1.

Station	1	2	3	4	5	6	Total
Station capacity	20	25	17	20	25	15	122
Initial inventory	15	23	8	17	16	9	88
Target inventory	5	11	7	16	18	9	66
Broken bikes	0	2	3	3	3	0	11

Table 4.18
Station information in Scenario 2 in Section 4.4.1.

Station	1	2	3	4	5	6	Total
Station capacity	20	25	17	20	25	15	122
Initial inventory	20	11	8	17	0	9	65
Target inventory	5	23	7	16	23	9	83
Broken bikes	0	2	3	3	3	0	11

distance matrix is the same as that in Scenario 1. The optimal solution in Scenario 2 is 0-5-1-4-2-3-5-0.

It can be seen from Table 4.18 that Station 5 is in need of 23 usable bikes, which is larger than the vehicle capacity (20 bikes). Therefore, Station 5 is visited twice, with the first and second visits dropping off 18 and 5 usable bikes, respectively.

4.4.2. Multiple visits due to broken bikes

The difference in handling between usable and broken bikes is that the usable bikes can be transferred among stations whereas broken bikes stay on the vehicle all the way to the depot. Therefore, the emissions contributed by a broken bike on average are larger than those by a usable bike and it is wise to drop off broken bikes by visiting the depot whenever possible. Thus, in some cases, although the vehicle capacity is enough to handle both types of bikes in one tour, the vehicle still goes back to the depot to drop broken bikes in order to reduce the load and hence the emissions. An example is provided using the station and distance information shown in Table 4.19 and Table 4.20, respectively.

Table 4.21 provides the solution details. The second row named “Multi-visit to the depot” is the optimal solution provided by CPLEX, where multiple visits are allowed. The optimal vehicle route has 9 stops in total, including the start and the end, and has one extra visit to the depot halfway. Other stations are visited exactly once. The average load over 8 links is 6.75. The total distance of the whole route is 4.8 km and the vehicle generates 4.113 kg of CO_2 emissions. The third row named “Single-visit to the depot” is the case that the extra visit to the depot is manually deleted. It can be found that the optimal solution with a single visit to the depot also complies with the capacity constraint. However, the average load increases by 77.78%. Although the single-visit case reduces the distance by 4.17% compared with the multiple-visit counterpart, the emissions increase by 2.21%.

The different trend between the distance and emissions is due to the fundamental definition of emissions — the emissions are determined by not only travel distance but also vehicle loads. If the extra visit to the depot is eliminated, the number of stops is reduced by 1. However, this elimination is associated with an additional fixed load to all the links after the depot. This fixed load equals the number of broken bikes on the vehicle before visiting the depot. Therefore, the vehicle will have an extra visit to the depot if the emissions caused by those loads are larger than those caused by going back to the depot.

4.4.3. Multiple visits due to emission minimization

In some cases, the demand of a specific station can be satisfied by a single visit. However, in order to reduce the emissions, the vehicle may visit this station twice although sometimes at the cost of a longer travel distance. The station information shown in Table 4.22 and the distance information given in Table 4.23 are used as an example of this situation.

Table 4.24 provides the solution for this example. The second row is the optimal solution where multiple visits are permitted. In the optimal route, Station 3 is visited twice by the vehicle. There are 9 stops in total and the average load over 8 links is 7.25. The total distance of the whole route is 4.5 km and the CO_2 emissions are 3.821 kg. However, the demand of Station 3 is actually less than the vehicle capacity, which means that its demand can be covered within one visit, as shown in the third row of Table 4.24. For the single-visit case where the extra visit to Station 3 is manually deleted, the vehicle loads are within the vehicle capacity after every

Table 4.19
Station information for multiple visits due to broken bikes.

Station	1	2	3	4	5	6	Total
Station capacity	20	25	17	20	25	15	122
Initial inventory	11	11	9	13	8	9	61
Target inventory	8	9	5	20	12	7	61
Broken bikes	2	2	3	5	3	4	19

Table 4.20
Travel distances (in hundred meters) between stations for multiple visits due to broken bikes.

	Depot	1	2	3	4	5	6
Depot	0	12	10	5	8	2	4
1	10	0	17	10	4	13	13
2	9	15	0	9	16	7	9
3	12	10	11	0	12	6	12
4	7	6	14	9	0	9	9
5	2	12	7	8	12	0	4
6	4	15	9	9	9	6	0

Table 4.21
Solutions for multiple visits due to broken bikes.

	Vehicle route	Loads on the vehicle	Average load	Distance (km)	Emissions (kg)
Multi-visit to the depot	0-3-1-4-0-6-2-5-0	0-7-12-10-0-6-10-9-0	6.75	4.8	4.113
Single-visit to the depot	0-3-1-4-6-2-5-0	0-7-12-10-16-20-19-0	12	4.6	4.204
Change (%)	-	-	+77.78	−4.17	+2.21

Table 4.22
Station information for multiple visits due to emission minimization.

Station	1	2	3	4	5	6	Total
Station capacity	20	25	17	20	25	15	122
Initial inventory	16	20	14	7	15	3	75
Target inventory	18	12	0	20	21	4	75
Broken bikes	1	2	1	3	2	1	10

Table 4.23
Travel distances (in hundred meters) between stations for multiple visits due to emission minimization.

	Depot	1	2	3	4	5	6
Depot	0	12	14	4	9	12	13
1	6	0	8	6	7	13	5
2	12	11	0	11	8	3	13
3	11	7	15	0	6	7	7
4	9	10	10	6	0	9	12
5	14	2	9	15	11	0	12
6	15	9	15	7	12	10	0

Table 4.24
Solution for multiple visits due to emission minimization.

	Vehicle route	Loads on the vehicle	Average load	Distance (km)	Emissions (kg)
Multi-visit to a station	0-3-6-3-4-2-5-1-0	0-1-1-15-5-15-11-10-0	7.25	4.5	3.821
Single-visit to a station	0-3-6-4-2-5-1-0	0-15-15-5-15-11-10-0	10.14	4.4	3.966
Change (%)	–	–	+39.86	−2.22	+3.79

stop. However, the average load increases by 39.86% compared with the multi-visit case and the emissions increase by 3.79% although the travel distance can be reduced by around 2.22%.

This example shows the impact of vehicle loads on emissions. In this example, a longer distance leads to fewer emissions. The reason is that the emission function (2) actually assigns a 'weight' to each link distance, whose value increases with the vehicle load on this link. According to the emission function (2), emissions are composed of two parts: the sum of travel distances and the sum of the product of load and distance, each having a coefficient. A shorter route can lead to a larger sum of the product of load and distance, leading to larger emissions.

4.4.4. Summary

Multiple visits are essential in balancing a BSS. First, when a perfect balance is required and the total supply of all stations is larger than the vehicle capacity, a vehicle may need to go back to the depot halfway. Alternatively, the demand of a single station is larger than the vehicle capacity, a vehicle is required to visit this station twice or more to satisfy the demand. Second, a vehicle can go back

Table 4.25
Solutions under different vehicle capacities.

		Optimal route	Loads on the vehicle	Number of stops	Emissions (kg)
Vehicle capacity Q	10	0-2-5-3-2-0-1-3-2-6-1-4-0	9-0-8-10-5-10-0-10-3-8-8-8-0	13	8.460
	15	0-1-3-2-5-0-2-6-1-4-0	13-0-12-4-12-13-0-5-8-8-0	11	6.710
	20	0-2-6-3-2-5-0-1-4-0	10-0-5-17-6-14-16-6-6-0	10	5.824
	25	0-2-6-3-1-5-4-0	25-4-9-21-11-19-19-0	8	5.465
	30	0-2-6-3-1-4-5-0	26-5-10-22-12-12-20-0	8	4.995
	35	0-2-6-3-1-4-5-0	26-5-10-22-12-12-20-0	8	4.995
	40	0-2-6-3-1-4-5-0	26-5-10-22-12-12-20-0	8	4.995
	45	0-2-6-3-1-4-5-0	26-5-10-22-12-12-20-0	8	4.995
	1000	0-2-6-3-1-4-5-0	26-5-10-22-12-12-20-0	8	4.995

to the depot halfway to unload all broken bikes and collect some usable bikes at the depot so that it can carry fewer usable bikes at the first departure from the depot and along the journey after the second visit of the depot, leading to lower the emissions generated. Third, the demand of a station can be satisfied over multiple visits to reduce the vehicle loads and hence the emissions.

4.5. The effect of vehicle capacity

This section will investigate the effect of vehicle capacity on the emissions. Following the study of Erdoğan et al. (2015), we carried out the experiments using the data in the base scenario with $Q \in \{10, 15, 20, 25, 30, 35, 40, 45, 1000\}$. We assume that the fuel consumption induced by one unit increase in the vehicle load is fixed for all scenarios. The corresponding results are shown in Table 4.25.

When the vehicle capacity is only 10, the optimal route has 13 stops in total and an extra visit to the depot halfway. Station 2 is visited three times and Stations 1 and 3 are visited twice. The emissions are 8.460 kg. When the capacity increases to 15, the optimal route changes greatly compared with the former case. The number of stops is reduced by 2 and the emissions decrease to 6.710 kg. The number of stops keeps decreasing before the capacity increases to 25, in which case the depot is not visited halfway during the journey. After that, the number of stops remains at 8, and the emissions remain at 4.995 kg. When the vehicle capacity is far more than the station demand (i.e., the capacity is set as 1000), the emissions are still 4.995 kg. It can be found that in this case, when the vehicle capacity is larger than 30, the capacity has no effect on the optimal solutions. Theoretically, when the vehicle capacity is equal to or larger than 26, the capacity has no effect on the optimal solution, because the load on the vehicle is no longer affected by the capacity.

In summary, when the vehicle capacity increases, the CO_2 emissions and the number of stops are non-increasing functions of the vehicle capacity. The route and vehicle load may be adjusted due to the change in the vehicle capacity. However, when the capacity exceeds a certain value, it will have no effect on the optimal solutions.

4.6. Comparison between emission and distance minimization solutions

This section will compare emission and distance minimization solutions. The mathematical model for distance minimization is the same that as shown in Section 3 except for the objective function. We used the data in the benchmark instances created by Rainer-

Table 4.26
Comparison between emission and distance minimization solutions.

Instance	Characteristics of the optimal solution	Emission minimization	Distance minimization	Change
S10B10_00	Emission (kg)	25.334	25.334	25.334
	Distance (km)	29.0	28.6	−1.38%
	No. of stops	12	12	0.00%
S10B10_06	Emission (kg)	23.807	24.865	4.44%
	Distance (km)	27.8	26.4	−5.04%
	No. of stops	11	11	0.00%
S10B10_12	Emission (kg)	23.975	24.662	2.87%
	Distance (km)	26.8	26.3	−1.87%
	No. of stops	12	12	0.00%
S10B10_18	Emission (kg)	24.403	25.967	6.41%
	Distance (km)	27.9	27.6	−1.08%
	No. of stops	12	12	0.00%
S10B10_24	Emission (kg)	20.994	21.708	3.40%
	Distance (km)	23.7	23.1	−2.53%
	No. of stops	12	12	0.00%

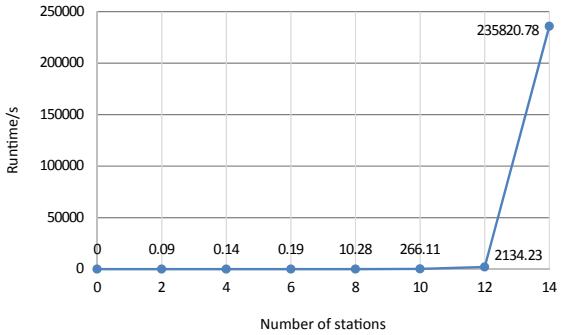

Fig. 4.3. Runtime against the number of stations.

Harbach et al. (2015) based on Citybike Vienna. Five instances with 10 stations were then selected as shown in the first column of Table 4.26 and 10% broken bikes were randomly distributed among stations. The name of each instance is formatted as ["S"][Number of stations]["B"][Percentage of broken bikes]_[Counter in the dataset]. For example, "S10B10_00" is an instance numbered as "00" in the dataset with 10 stations and 10% of the bikes are broken. The results are shown in Table 4.26. For different objectives, i.e., emission minimization or distance minimization, the characteristics of the optimal solution are presented, including the total emissions, total travel distance, and the number of stops. The last column shows the changes in the corresponding characteristics obtained under distance minimization with respect to emission minimization.

Based on the instances shown in Table 4.26, the optimal solutions under distance minimization generally have shorter travel distances but larger emissions than those under emission minimization. There is no change in the number of stops, which implies that no multiple visits are triggered due to emission minimization in this example. Moreover, the difference in solutions under two objectives indicates that a shorter distance may not necessarily lead to lower emissions.

4.7. Model and clustering performance

This section will illustrate the performance including the runtime complexity of the proposed model under single- and multiple-vehicle cases, and provide an alternative—clustering before using an exact method—in solving large network instances. The runtime performance and solution quality obtained by this alternative will also be demonstrated. The data in the benchmark instances created by Rainer-Harbach et al. (2015) are adopted here.

To show the runtime performance of the proposed model, the number of stations increased from 0 to 14 at regular intervals equal to 2. For each number of stations, the runtime was recorded under the tightest value of A, i.e., the number of stops in the optimal solution. The relationship between the runtime and the number of stations is shown in Fig. 4.3.

It can be found that when the number of stations is 10 or less, the model can be solved within less than 5 min. However, when the number of stations increases to 12, the model requires much more runtime to be solved. When there are 14 stations, the problem cannot be solved within two hours. It implies that for larger network instances, it is intractable to solve the model using exact methods in a reasonable running time. It is because the decision variable x_{iak} has three dimensions. The number of variables equals $A \cdot |S| \cdot |V|$. If the number of vehicles is fixed, when the number of stations increases, the upper bound A also increases. Moreover, $|S|$ is larger when the number of stations is larger. Therefore, $A \cdot |S|$ and the number of variables are nonlinear functions of the number of stations, which leads to the nonlinear trend in the runtime.

For the multiple-vehicle case, we used the instance "S10B10_00" mentioned in Section 4.6 to compare the solutions under different numbers of vehicles. The results are shown in Table 4.27, including the optimal routes, the total emissions of all vehicles employed, and the runtime. It can be observed that when the number of vehicles increases, the total emissions increase and so does the runtime.

One possible approach to overcoming the time complexity issue for solving a realistic large network instance is to decompose the large network into several clusters, assign one vehicle to each cluster, develop a model for each cluster based on the formulation in Section 3, and finally solve each model by CPLEX sequentially (e.g., Forma et al., 2015; Brinkmann et al., 2016; Schuijbroek et al.,

Table 4.27
Optimal solutions and the corresponding runtimes under different numbers of vehicles.

Number of vehicles	Optimal routes	Total emissions (kg)	Runtime (s)
1	0-8-6-9-2-4-1-10-3-5-7-0	25.334	266.11
2	0-6-8-3-5-7-0 0-9-2-4-1-10-0	27.907	495.09
3	0-3-9-2-0 0-5-7-4-0 0-6-8-1-10-0	30.609	20541.76

Table 4.28
Optimal routes in all the clusters.

Cluster	Optimal route
1	0-59-36-39-0-89-18-22-2-0
2	0-11-51-56-84-88-77-35-0
3	0-14-53-76-58-40-42-6-0
4	0-28-23-0-46-68-41-54-27-0
5	0-26-62-86-70-55-44-24-0
6	0-33-50-45-19-65-13-4-0
7	0-43-83-75-82-79-69-0
8	0-21-29-57-47-60-9-0
9	0-1-31-67-63-12-5-17-0
10	0-80-81-72-71-78-74-90-0
11	0-3-7-16-73-64-61-8-0
12	0-32-34-87-85-38-25-30-0
13	0-66-37-52-48-20-15-0

2017; Ghosh et al., 2017). A network having 90 stations is used to show the performance of this clustering approach. 10% of total bikes were assumed to be broken and distributed randomly among stations. 13 clusters were constructed in total using the nearest neighbor heuristic with each cluster having 6 to 7 stations and one depot. The clustering results and corresponding optimal routes are provided in Table 4.28. The total computing time is 11.42 s and the total emissions are 231.321 kg. This result confirms the possibility of using the clustering approach to reduce the running time for large network instances with multiple vehicles.

To compare the performance with and without using the clustering approach, 2 clusters were generated for the 12-station network using the nearest neighbor heuristic. The emissions of each cluster are 11.591 kg and 19.175 kg and the total amount is 30.766 kg. The computational time is 0.82 s. If the clustering approach was not used, the emissions are 28.666 kg and the computational time is more than half an hour as recorded in Fig. 4.3. It can be seen that although the solution quality is reduced, the computational time is improved significantly.

When the network size is 30, CPLEX is not able to converge to the optimal solution within a limit of 3 h. The feasible solution provided by CPLEX within 3 h gives 82.969 kg with a gap of 100.00%. If three clusters were created using the nearest neighbor heuristic, the solution gives 78.462 kg, which is 5.43% better than the emissions without clustering, but the computational time is less than half an hour.

The clustering results also relate to the number of stations in each cluster. Taking the 90-station network in Table 4.28 as an example, when the cluster size increases from 5 to 10 stations, the emissions have a decreasing trend in general as shown in Fig. 4.4 (a) but the runtime is a nonlinear increasing function of the cluster size (Fig. 4.4b).

Different clustering methods exist and can be used before applying the exact method for the BRP. The solutions also depend on the clustering method adopted. For example, if we used the insertion heuristic to generate 13 clusters for the same 90-station network as in Table 4.28, the optimal emissions are 235.936 kg (about 2% worse than the solution of the nearest neighbor heuristic) and the computational time is 24.2 s (more than doubled the running time of the nearest neighbor heuristic). Schuijbroek et al. (2017) also provided another option for clustering, which was derived based on the problem's properties. We believe that more effective clustering methods can be developed to obtain better solutions to our proposed problem. Indeed, developing more effective clustering techniques for our problem is an important research topic that deserves a full investigation. This is left for future research.

5. Discussion

Other than the clustering approach used in Section 4.7, there are at least three approaches to solving a large scale BRP. One approach is to incorporate well-known decomposition techniques (e.g., Largangian, Benders, Dantzig-Wolfe) into exact methods to get global optima. For example, Erdoğan et al. (2014, 2015) used Benders decomposition together with a branch-and-cut algorithm to solve the static BRP with the objective of cost minimization. They showed that the method can solve the instances with up to 60 stations. Contardo et al. (2012) used Dantzig-Wolfe and Benders decomposition to efficiently find the lower and upper bounds for the branch-and-bound algorithm for a dynamic BRP with the objective of unmet demand minimization. The key challenge for using this approach to solving our proposed problem with multiple vehicles to optimality is to identify the problem structure so that the subproblem can be solved to optimality efficiently. This is left for future research.

An alternative approach to solving a large scale BRP is to decompose the whole problem into different specific subproblems, such as a routing problem (i.e., the problem of finding the route of each vehicle) and a loading subproblem (i.e., the problem of finding loading and unloading quantities at each visited station for each vehicle). Each subproblem is then solved by exact methods, heuristics, or metaheuristics (with local search incorporated) (see e.g., Forma et al., 2015; Brinkmann et al., 2016). The main challenge for using this approach to solving our proposed problem with multiple vehicles is to ensure that after the decomposition, all the subproblems can be either solved to optimality by exact methods or solved by heuristics/metaheuristics efficiently. This is left to future studies.

One more approach is to develop heuristics or metaheuristics to solve the whole problem without decomposition or clustering. The major challenge is to identify the problem properties that can help to perform local search quickly. The authors are going to use this approach to overcome the time complexity issue of the multiple vehicle case. The methodology will be reported in another paper.

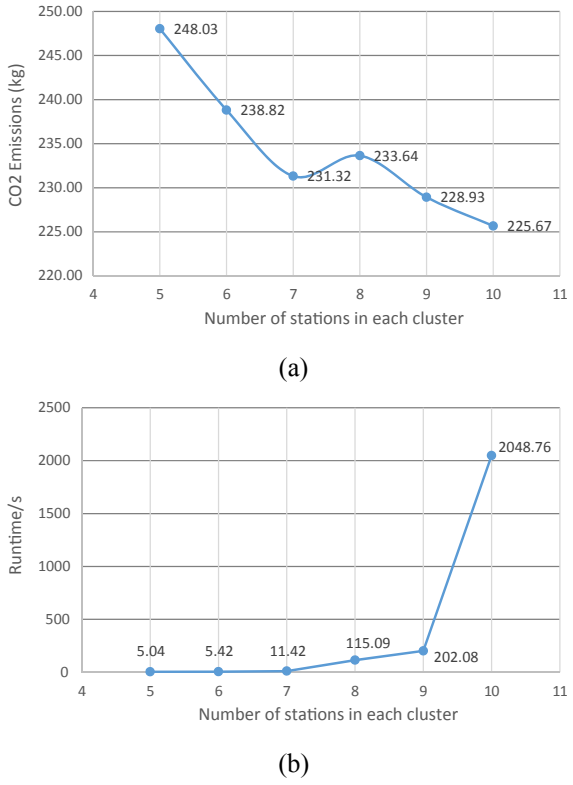

Fig. 4.4. The changes in the objective value and the computational time when increasing the cluster size: (a) CO_2 emissions in kg, (b) computational time in seconds.

6. Conclusion

This study has tackled a repositioning problem in a BSS with broken bikes. In addition to shipping usable bikes among stations and the depot by multiple fossil-fuelled vehicles to achieve a perfect balance between bike demand and supply at each station, the operator also needs to transport broken bikes to the depot for repairs. Unlike most of the other existing BRPs, this problem is aimed to minimize the total CO_2 emissions of all repositioning vehicles. The emissions relate to not only the travel distance, which has been used as the objective in many studies, but also the loads on the vehicles. An MILP model is proposed to formulate this problem using the sequence-indexed formulation approach. Vehicle capacity is taken into consideration. CPLEX has been applied to determine the routing and loading decisions for the repositioning operation.

Small networks have been used in the numerical examples to illustrate the properties of the proposed model. Five possible dimensions are considered to analyze their effects on emissions, including the demand tolerance, the percentage of broken bikes, the distances between stations, multiple visits to the depot and stations, and vehicle capacity. The results indicate that if there is a tolerance for meeting the demand target, when this tolerance increases, the CO_2 emissions decrease. Moreover, increasing the percentage of broken bikes aggravates the emissions. Furthermore, the effect of link distance depends on whether it is in an optimal route. If it is not in the optimal route, the increase of link distance does not affect the CO_2 emissions. Otherwise, the increase in link distance often leads to an increase in the CO_2 emissions but the emissions may remain unchanged in some cases. In addition, allowing multiple visits can reduce vehicle emissions. Besides, employing larger vehicles can lead to lower emissions.

We have also used the data in the benchmark instances created by Rainer-Harbach et al. (2015) based on Citybike Vienna to compare emission and travel distance minimization solutions and the effect of the number of vehicles. The results indicate that a shorter distance may not necessarily lead to lower emissions. The results also show that as the number of vehicles increases, the total emissions and runtime increase. For large network instances with multiple vehicles, we used a clustering method based on the nearest neighbor heuristic to decompose the network into several groups, each of which was tackled sequentially using the proposed model together with CPLEX. This result illustrates the performance of this solution approach and confirms the possibility of using the clustering approach to reduce the running time for large network instances with multiple vehicles. Further developments will be on meta-heuristics, which can provide satisfactory results within a reasonable time, even for large network instances with multiple vehicles. Solving the proposed problem using decomposition techniques can be a good future research direction. Developing a clustering technique that can give better solutions to our proposed problem than classical geographical clustering techniques is another research direction.

Acknowledgments

This research was supported by a grant from the National Natural Science Foundation of China (No. 71771194). The authors are grateful to the three reviewers for their constructive comments.

References

Alvarez-Valdes, R., Belenguer, J.M., Benavent, E., Bermudez, J.D., Muñoz, F., Vercher, E., Verdejo, F., 2016. Optimizing the level of service quality of a bike-sharing system. Omega 62, 163–175.
Angeloudis, P., Hu, J., Bell, M.G.H., 2014. A strategic repositioning algorithm for bicycle-sharing schemes. Transportmet. A: Transp. Sci. 10 (8), 759–774.
Benchimol, M., Benchimol, P., Chappert, B., De La Taille, A., Laroche, F., Meunier, F., Robinet, L., 2011. Balancing the stations of a self service “Bike hire” system. RAIRO – Operat. Res. 45, 37–61.
Brinkmann, J., Ulmer, M.W., Mattfeld, D.C., 2015. Short-term strategies for stochastic inventory routing in bike sharing systems. Transp. Res. Procedia 10, 364–373.
Brinkmann, J., Ulmer, M.W., Mattfeld, D.C., 2016. Inventory routing for bike sharing systems. Transp. Res. Procedia 19, 316–327.
Caggiani, L., Ottomanelli, M., 2012. A modular soft computing based method for vehicles repositioning in bike-sharing systems. Procedia-Social Behav. Sci. 54, 675–684.
Caggiani, L., Camporeale, R., Ottomanelli, M., Szeto, W.Y., 2018. A modeling framework for the dynamic management of free-floating bike-sharing systems. Transport. Res. Part C: Emerg. Technol. 87, 159–182.
Chemla, D., Meunier, F., Wolfler Calvo, R., 2013. Bike sharing systems: solving the static rebalancing problem. Discrete Optimiz. 10 (2), 120–146.
Contardo, C., Morency, C., Rousseau, L.-M., 2012. Balancing a dynamic public bike-sharing system. Technical Report CIRRELT-2012-09. CIRRELT, Montreal, Canada.
Cruz, F., Subramanian, A., Bruck, B.P., Iori, M., 2017. A heuristic algorithm for a single vehicle static bike sharing rebalancing problem. Comput. Oper. Res. 79, 19–33.
Dell’Amico, M., Hadjicostantinou, E., Iori, M., Novellani, S., 2014. The bike sharing rebalancing problem: mathematical formulations and benchmark instances. Omega 45, 7–19.
Dell’Amico, M., Iori, M., Novellani, S., Stützle, T., 2016. A destroy and repair algorithm for the bike sharing rebalancing problem. Comput. Oper. Res. 71, 149–162.
Demir, E., Bektaş, T., Laporte, G., 2011. A comparative analysis of several vehicle emission models for road freight transportation. Transport. Res. Part D: Transp. Environ. 16 (5), 347–357.
Demir, E., Bektaş, T., Laporte, G., 2012. An adaptive large neighborhood search heuristic for the pollution-routing problem. Eur. J. Oper. Res. 223 (2), 346–359.
Di Gaspero, L., Rendl, A., Urli, T., 2013. A hybrid ACO + CP for balancing bicycle sharing systems. In: Hybrid Metaheuristics. Lecture Notes in Computer Science 7919. Springer, Berlin Heidelberg, pp. 198–212.
Di Gaspero, L., Rendl, A., Urli, T., 2016. Balancing bike sharing systems with constraint programming. Constraints 21 (2), 318–348.
Ehmke, J.F., Campbell, A.M., Thomas, B.W., 2016. Vehicle routing to minimize time-dependent emissions in urban areas. Eur. J. Oper. Res. 251 (2), 478–494.
Erdoğan, G., Laporte, G., Wolfler Calvo, R., 2014. The static bicycle relocation problem with demand intervals. Eur. J. Oper. Res. 238 (2), 451–457.
Erdoğan, G., Battarra, M., Wolfler Calvo, R., 2015. An exact algorithm for the static rebalancing problem arising in bicycle sharing systems. Eur. J. Oper. Res. 245 (3), 667–679.
Forma, I.A., Raviv, T., Tzur, M., 2015. A 3-step math heuristic for the static repositioning problem in bike-sharing systems. Transport. Res. Part B: Methodol. 71, 230–247.
Ghosh, S., Varakantham, P., 2017. Incentivising the use of bike trailers for dynamic repositioning in bike sharing systems. International Conference on Automated Planning and Scheduling (ICAPS).
Ghosh, S., Varakantham, P., Adulyasak, Y., Jaillet, P., 2017. Dynamic repositioning to reduce lost demand in bike sharing systems. J. Artific. Intell. Res. 58, 387–430.
Ho, S.C., Szeto, W.Y., 2014. Solving a static repositioning problem in bike-sharing systems using iterated tabu search. Transport. Res. Part E: Logist. Transport. Rev. 69, 180–198.
Ho, S.C., Szeto, W.Y., 2017. A hybrid large neighborhood search for the static multi-vehicle bike-repositioning problem. Transport. Res. Part B: Methodol. 95, 340–363.
Hosseini-Nasab, H., Lotfalian, P., 2017. Green routing for trucking systems with classification of path types. J. Clean. Prod. 146, 228–233.
Kaspi, M., Raviv, T., Tzur, M., 2016. Detection of unusable bicycles in bike-sharing systems. Omega 65, 10–16.
Kaspi, M., Raviv, T., Tzur, M., 2017. Bike-sharing systems: user dissatisfaction in the presence of unusable bicycles. IISE Trans. 49, 144–158.
Kloimüllner, C., Papazek, P., Hu, B., Raidl, G.R., 2014. Balancing bicycle sharing systems: an approach for the dynamic case. In: European Conference on Evolutionary Computation in Combinatorial Optimization. Springer, pp. 73–84.
Koç, Ç., Bektaş, T., Jabali, O., Laporte, G., 2014. The fleet size and mix pollution-routing problem. Transport. Res. Part B: Methodol. 70, 239–254.
Kopfer, H.W., Schönberger, J., Kopfer, H., 2014. Reducing greenhouse gas emissions of a heterogeneous vehicle fleet. Flexible Serv. Manuf. J. 26 (1–2), 221–248.
Li, Y., Szeto, W.Y., Long, J.C., Shui, C.S., 2016. A multiple type bike repositioning problem. Transp. Res. Part B 90, 263–278.
Lin, C., Choy, K.L., Ho, G.T.S., Chung, S.H., Lam, H.Y., 2014. Survey of green vehicle routing problem: past and future trends. Expert Syst. Appl. 41 (4), 1118–1138.
Meddin, R., DeMaio, P., 2018. The bike-sharing world map. Retrieved from http://www.bikesharingworld.com/ (access on 16 September 2018).
Nair, R., Miller-Hooks, E., Hampshire, R.C., Bušić, A., 2013. Large-scale vehicle sharing systems: analysis of Vélib'. Int. J. Sustain. Transport. 7 (1), 85–106.
O'Mahony, E., Shmoys, D.B., 2015. Data analysis and optimization for (Citi) bike sharing. In: Proceedings of the Twenty-Ninth AAAI Conference on Artificial Intelligence Data, pp. 687–694.
Papazek, P., Kloimüllner, C., Hu, B., Raidl, G.R., 2014. Balancing bicycle sharing systems: an analysis of path relinking and recombination within a GRASP hybrid. In: International Conference on Parallel Problem Solving from Nature 8672. Springer, Berlin Heidelberg, pp. 792–801.
Raidl, G.R., Hu, B., Rainer-Harbach, M., Papazek, P., 2013. Balancing bicycle sharing systems: improving a VNS by efficiently determining optimal loading operations. In: Hybrid Metaheuristics. Lecture Notes in Computer Science 7919. Springer, Berlin Heidelberg, pp. 130–143.
Rainer-Harbach, M., Papazek, P., Hu, B., Raidl, G.R., 2013. Balancing bicycle sharing systems: a variable neighborhood search approach. In: Evolutionary Computation in Combinatorial Optimization. Lecture Notes in Computer Science 7832. Springer, Berlin Heidelberg, pp. 121–132.
Rainer-Harbach, M., Papazek, P., Raidl, G.R., Hu, B., Kloimüllner, C., 2015. PILOT, GRASP, and VNS approaches for the static balancing of bicycle sharing systems. J. Global Optim. 63 (3), 597–629.
Raviv, T., Tzur, M., Forma, I.A., 2013. Static repositioning in a bike-sharing system: models and solution approaches. EURO J. Transport. Logist. 2 (3), 187–229.
Schuijbroek, J., Hampshire, R.C., Van Hoeve, W.-J., 2017. Inventory rebalancing and vehicle routing in bike sharing systems. Eur. J. Oper. Res. 257 (3), 992–1004.
Scott, C., Urquhart, N., Hart, E., 2010. Influence of topology and payload on CO_2 optimised vehicle routing. Applications of Evolutionary Computation 6025, 141–150.
Shui, C.S., Szeto, W.Y., 2018. Dynamic green bike repositioning problem – a hybrid rolling horizon artificial bee colony algorithm approach. Transport. Res. Part D: Transp. Environ. 60, 119–136.
Suzuki, Y., 2011. A new truck-routing approach for reducing fuel consumption and pollutants emission. Transport. Res. Part D: Transp. Environ. 16 (1), 73–77.
Szeto, W.Y., Liu, Y., Ho, S.C., 2016. Chemical reaction optimization for solving a static bike repositioning problem. Transp. Res. Part D 47, 104–135.
Szeto, W.Y., Shui, C.S., 2018. Exact loading and unloading strategies for the static multi-vehicle bike repositioning problem. Transport. Res. Part B: Methodol. 109, 176–211.
Ubeda, S., Arcelus, F.J., Faulin, J., 2011. Green logistics at Eroski: A case study. Int. J. Prod. Econ. 131 (1), 44–51.
Wiersma, B., 2010. Bicycle Sharing System: Role, Effects and Application to Plymouth. Masters, University of Groningen, Groningen.
Xiao, Y., Konak, A., 2016. The heterogeneous green vehicle routing and scheduling problem with time-varying traffic congestion. Transport. Res. Part E: Logist. Transport. Rev. 88, 146–166.
Xiao, Y., Zhao, Q., Kaku, I., Xu, Y., 2012. Development of a fuel consumption optimization model for the capacitated vehicle routing problem. Comput. Oper. Res. 39 (7), 1419–1431.
Zhang, D., Yu, C., Desai, J., Lau, H.Y.K., Srivathsan, S., 2017. A time-space network flow approach to dynamic repositioning in bicycle sharing systems. Transport. Res. Part B: Methodol. 103, 188–207.
Zhang, J., Zhao, Y., Xue, W., Li, J., 2015. Vehicle routing problem with fuel consumption and carbon emission. Int. J. Prod. Econ. 170, 234–242.
Zhang, S., Lee, C.K.M., Choy, K.L., Ho, W., Ip, W.H., 2014. Design and development of a hybrid artificial bee colony algorithm for the environmental vehicle routing problem. Transport. Res. Part D: Transp. Environ. 31, 85–99.